Chin. J. Astron. Astrophys. Vol. 1, No. 4, (2001) 349–356
(http://www.chjaa.org or http://chjaa.bao.ac.cn)

Chinese Journal of
Astronomy and
Astrophysics

Hydrodynamic Evolution of GRB Afterglow

Ji-Rong Mao⋆ and Jian-Cheng Wang

Yunnan Observatory, Chinese Academy of Sciences, Kunming 650011
National Astronomical Observatories, Chinese Academy of Sciences, Beijing 100012
United Laboratory of Optical Astronomy, Chinese Academy of Sciences

Received 2001 January 19; accepted 2001 June 23

Abstract We investigate the dynamics of a relativistic fireball which decelerates as it sweeps up ambient matter. Not only the radiative and adiabatic cases, but also the realistic intermediate cases are calculated. We perform numerical calculation for various ambient media and sizes of beaming expansion, and find that the deceleration radius R_0 may play an important role for the hydrodynamic evolution of GRB afterglow.

Key words: gamma-rays: bursts — hydrodynamics – shock waves

1 INTRODUCTION

From the detection at X-ray, optical and radio wavelengths of gamma-ray bursts (GRBs) since 1997 (Costa et al. 1997; van Paradijs et al. 1997; Sahu et al. 1997; Djorgovski et al. 1997; Metzger et al. 1997; Frail et al. 1997; Taylor et al. 1997; Kulkarni et al. 1998; Halpern et al. 1998; Castro-Tirado et al. 1999; Kulkarni et al. 1999; Galama et al. 1999), we have come to know that the GRBs can release $10^{51} \sim 10^{54}$ ergs in a few seconds and that the fireball model can describe these emissions well. When the fireball/blast-wave shock (Rees & Mészáros 1992; Mészáros & Rees 1993; Mészáros, Laguna & Rees 1993; Panaitescu & Mészáros 1998) sweeps up the surrounding ambient medium, radiation in X-ray, optical and radio bands, called afterglow, is produced. Because the hydrodynamic evolution of the fireball model primarily determines the properties of the observed light curves and spectra in the afterglow, we should investigate the evolution comprehensively.

Nearly all the previous literature assumes that when the blast wave sweeps up the surrounding medium, the hydrodynamic evolution is either adiabatic or radiative. Both these cases have been studied (Mészáros & Rees 1997; Wijers, Rees & Mészáros 1997; Waxman 1997a, 1997b; Katz & Piran 1997; Dai & Lu 1998; Sari, Piran & Narayan 1998; Panaitescu, Mészáros & Rees 1998; Huang et al. 1998; Huang, Dai & Lu 1998). However, the actual physical process should be neither purely adiabatic nor radiative. It is necessary to calculate the cases intermediate between the two limiting cases.

⋆ E-mail: mjr@cosmos.ynao.ac.cn

The standard model assumes that the density of the homogeneous medium is about $1\,\mathrm{cm}^{-3}$ and that the fireball is spherical. Recently, several authors (Chevalier & Li 1999; Panaitescu & Mészáros 1999; Dai & Lu 1999; Dai & Lu 2000a, 2000b; Moderski, Sikora & Bulik 2000; Kumar & Panaitescu 2000) considered the effects of a dense inhomogeneous medium and an anisotropic, beaming expansion on the fireball evolution. But these authors have not systematically calculated the complete process and nor compared the results for different physical conditions.

In this paper, we study the hydrodynamic evolution of the fireball under the effects of radiative efficiency, medium environment and anisotropic beaming expansion in detail. We present the physical processes and the basic equations of the hydrodynamic evolution in Section 2. In Section 3, we numerically calculate the hydrodynamic evolution from the basic equations and obtain the main results taking into account the effects of wind and beaming. In Section 4, we summarize our conclusions.

2 HYDRODYNAMIC EQUATIONS

2.1 Basic Equations

The main problem of the hydrodynamic evolution of the fireball is how the Lorentz factor $\Gamma(r)$ evolves with the radius r measured in the lab frame. As the external shock sweeps up the surrounding medium, its bulk kinetic energy is partly converted into internal kinetic energy of the medium. We assume that some fraction, ε_e, of the kinetic energy is injected directly into non-thermal electrons. Then we have two basic equations (Blandford & Mckee 1976; Chiang & Dermer 1998) from the energy and momentum conservation of relativistic shock wave, namely,

$$\frac{\mathrm{d}M}{\mathrm{d}r} = \rho(r)A(r)[(\Gamma(r)-1)(1-\varepsilon_e)+1], \tag{1}$$

$$\frac{\mathrm{d}\Gamma}{\mathrm{d}m} = -\frac{\Gamma^2-1}{M}, \tag{2}$$

where M is the total mass, $\mathrm{d}m = A(r)\rho(r)\mathrm{d}r$ the rest mass of the shock swept-up in a distance $\mathrm{d}r$, and $A(r)$ a cross-sectional area. From Equations (1) and (2), we have the third basic equation

$$M = M_0\left(\frac{\Gamma+1}{\Gamma_0+1}\right)^{\varepsilon_e-\frac{1}{2}}\left(\frac{\Gamma-1}{\Gamma_0-1}\right)^{-\frac{1}{2}}, \tag{3}$$

where $M_0 = 10^{-4}M_\odot$ is the initial mass of the shock shell, $\Gamma_0 = 100$ is the initial Lorentz factor.

We assume that the density of the medium has the profile

$$\rho = \rho_0\left(\frac{r}{r_0}\right)^{-k} = n_0 m_\mathrm{p}\left(\frac{r}{r_0}\right)^{-k}, \tag{4}$$

where m_p is the rest mass of proton, r_0 the initial radius as the fireball becomes the optically thin plasma that produces the gamma-ray bursts. k, a numerical parameter, can be 0, 1.5 or 2, its physical meaning will be explained in the next section. So r_0 is calculated by

$$M_0 = 4\pi r_0^2 \Delta L n m_\mathrm{p}, \tag{5}$$

$$\sigma_T n \Delta L = 1, \tag{6}$$

where ΔL is the length of the shock shell, σ_T the Thomson section. Then the radius r_0 is given by

$$r_0 = \left(\frac{\sigma_T M_0}{4\pi m_{\rm p}}\right)^{\frac{1}{2}} \simeq 10^{13}\,{\rm cm}\,. \tag{7}$$

From Equations (2) and (3), we have

$$\frac{{\rm d}\Gamma}{{\rm d}r} = -\frac{n_0 m_{\rm p}}{M_0} A(r)(\frac{r}{r_0})^{-k}(\Gamma^2-1)^{\frac{3}{2}}(\Gamma+1)^{-\varepsilon_e}(\Gamma_0^2-1)^{-\frac{1}{2}}(\Gamma_0+1)^{\varepsilon_e}\,. \tag{8}$$

When the mass of swept-up matter is equal to the initial mass of the shock shell, there is a deceleration radius R_0 defined by

$$M_0 = \int_{r_0}^{R_0} \Gamma_0 A(r)\rho(r){\rm d}r. \tag{9}$$

The deceleration radius R_0 will be calculated for various cases of dense medium environment and anisotropic beaming expansion. Equation (8) will be calculated numerically.

2.2 Wind Environment and Beaming Effect

If the shock shell is spherical, then we have

$$A(r) = 4\pi r^2\,. \tag{10}$$

Using Equations (4) and (10), noting $R_0 \gg r_0$, we get

$$R_0 = \left[\frac{(3-k)M_0}{4\pi n_0 m_{\rm p}\Gamma_0 r_0^k}\right]^{\frac{1}{3-k}}\,, \tag{11}$$

where $k=0$, $n_0 = 1.0\,{\rm cm}^{-3}$ is the case of homogeneous medium, $k=1.5$, $n_0 = 10^6\,{\rm cm}^{-3}$ is the case of wind in a typical red supergiant star (Fransson, Lundguist & Chevalier 1996) and $k=2$, and $n_0 = 10^6\,{\rm cm}^{-3}$ is that of a typical Wolf-Rayet star (Chevalier & Li 1999). For $k=0$ and $n_0 = 1.0\,{\rm cm}^{-3}$, the deceleration radius R_0 is about $7\times10^{16}\,{\rm cm}$. For $k=2$ and $n_0 = 3\times10^6\,{\rm cm}^{-3}$ (Dai 2000), the deceleration radius R_0 is about $3\times10^{18}\,{\rm cm}$.

We define

$$\chi = \frac{r}{R_0}\,, \tag{12}$$

and then Equation (8) can be rewritten as

$$\frac{{\rm d}\Gamma}{{\rm d}\chi} = -\frac{(3-k)}{\Gamma_0}\chi^{2-k}(\Gamma^2-1)^{\frac{3}{2}}(\Gamma+1)^{-\varepsilon_e}(\Gamma_0^2-1)^{-\frac{1}{2}}(\Gamma_0+1)^{\varepsilon_e}\,. \tag{13}$$

Obviously, $\varepsilon_e = 1$ is the radiative limit and $\varepsilon_e = 0$ is the adiabatic limit and these have been discussed in many papers when interpreting the light curve and spectrum of the afterglow.

If we take into account the beaming expansion of the fireball, then the cross-sectional area of the shock wave is given by

$$A(r) = \Omega_j r^2, \tag{14}$$

where Ω_j is the solid angle of the shock wave. As a result of the lateral expansion due to the properties of the thermodynamics (Rhoads 1997; Rhoads 1999; Sari, Piran & Halpern 1999), the value of Ω_j is not constant but increases with the radius. Here, we assume

$$\Omega_j = \left(\frac{r}{r_0}\right)^p \Omega_0, \tag{15}$$

$$\Omega_0 = 2\pi(1 - \cos\theta_0)\,. \tag{16}$$

The parameter p indicates the degree of the beaming effect. And the deceleration radius is given by

$$R_0 = \left[\frac{(3+p-k)M_0}{\Gamma_0\Omega_0 n_0 m_\mathrm{p} r_0^{k-p}}\right]^{\frac{1}{3+p-k}}\,. \tag{17}$$

Using Equation(12), we have the equation of the fireball evolution in the case of beaming expansion,

$$\frac{d\Gamma}{d\chi} = -(3+p-k)\frac{\chi^{P+2-k}}{\Gamma_0}(\Gamma^2-1)^{\frac{3}{2}}(\Gamma+1)^{-\varepsilon_e}(\Gamma_0^2-1)^{-\frac{1}{2}}(\Gamma_0+1)^{\varepsilon_e}. \tag{18}$$

Equations (13) and (18) are suitable not only for the radiative or adiabatic cases, but also for the more realistic cases.

3 NUMERICAL RESULTS

We solve the differential Equations (13) and (18) numerically. In Equation (13), there are two parameters, k and ε_e. As mentioned above, the case of $k = 0$ and $n_0 = 1.0\,\mathrm{cm}^{-3}$ corresponds to the environment of interstellar medium (ISM), $k = 1.5$ and $n_0 = 10^6\,\mathrm{cm}^{-3}$ is the case of wind in red supergiant star, and $k = 2$ and $n_0 = 10^6\,\mathrm{cm}^{-3}$ is that in Wolf-Rayet star. The parameter ε_e measures the fraction of the total thermal energy which goes into non-thermal electrons.

Here, we regard ε_e as a free parameter. Obviously, $0 \le \varepsilon_e \le 1$. $\varepsilon_e = 1$ is the radiative limit and $\varepsilon_e = 0$ is the adiabatic limit. $\varepsilon_e = 1/3$ corresponds to the case of equipartition among protons, electrons and magnetic field energy density (Ghisellini, Celotti & Lazzati 1999). $\varepsilon_e = 1/2$ corresponds to the case of maximum efficiency for the shock acceleration of electrons (Sari, Narayan & Piran 1996).

Fixing one of the parameters k and ε_e, we obtain the distance profile of the bulk Lorentz factor $\Gamma(r)$ as a function of the other parameter. We solve the Equation (13) and get the main results. Figure 1 displays the $\varepsilon_e = 1$ (radiative), $\varepsilon_e = \frac{1}{2}$, $\varepsilon_e = \frac{1}{3}$ and $\varepsilon_e = 0$ (adiabatic) cases. The results of homogeneous and inhomogeneous environments are compared in (a), (b), (c) and (d), respectively. Figure 2 shows the results in the homogeneous and inhomogeneous environments, and the cases of different values of ε_e are compared in (a), (b) and (c). Both Fig. 1 and Fig. 2 refer to the isotropic case.

Equation (18) have three parameters, k, ε_e and p. The meaning of k and ε_e has been explained. The parameter p indicates the degree of the beaming effect. We consider three values, $p = 0.5, 1, 2$. The results of Equation (18) are the hydrodynamic evolution in different environments with different size beaming effect. Since the results of different ε_e have been shown in Fig. 1 and Fig. 2, we now only show the results for $\varepsilon_e = \frac{1}{2}$. In Fig. 3, the isotropic case and the different cases of beaming (different value of p) are compared.

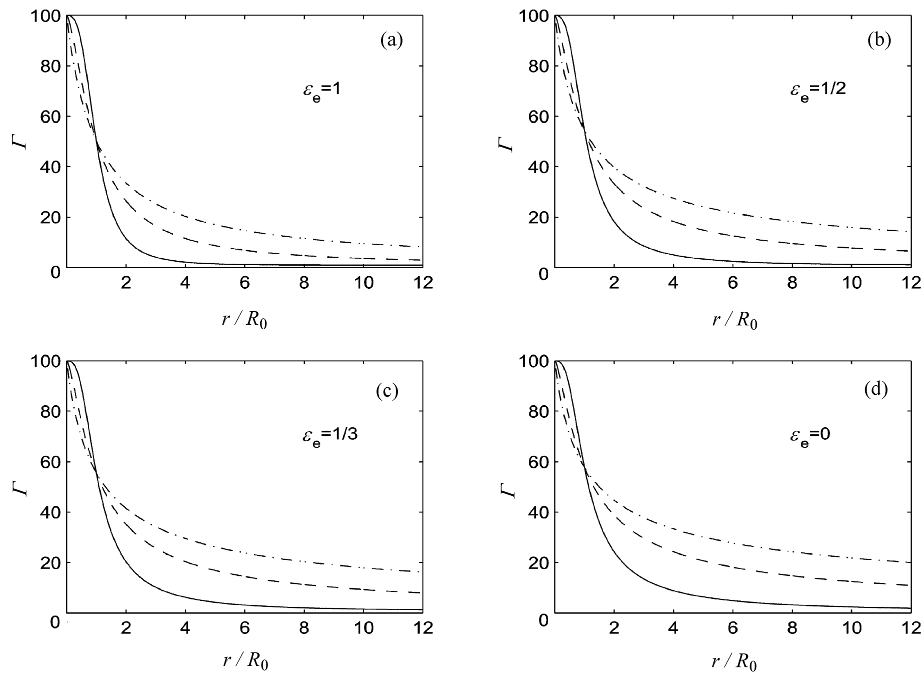

Fig. 1 The hydrodynamic evolution for various values of ε_e. Solid lines for $k = 0$, $n_0 = 1.0\,\mathrm{cm}^{-3}$, dashed lines for $k = 1.5$, $n_0 = 10^6\,\mathrm{cm}^{-3}$, dot-dash lines for $k = 2$, $n_0 = 10^6\,\mathrm{cm}^{-3}$.

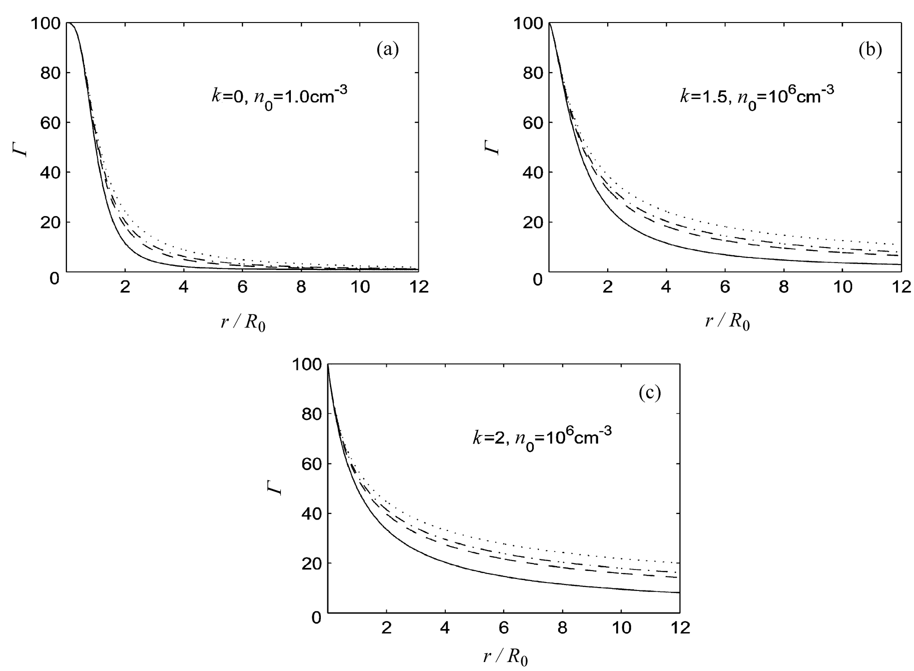

Fig. 2 The hydrodynamic evolution in different environments. Solid lines for $\varepsilon_e = 1$, dashed lines for $\varepsilon_e = \frac{1}{2}$, dot-dash lines for $\varepsilon_e = \frac{1}{3}$, dotted lines for $\varepsilon_e = 0$.

4 DISCUSSION AND CONCLUSIONS

There are two populations of GRBs: short-duration bursts and long-duration bursts. Short-duration bursts are the results of neutron star-neutron star mergers or black hole-neutron star mergers while the long-duration bursts are mostly dominated by the collapse of massive stars (Fryer, Woosley & Hartmann 1999). Since the long-duration bursts associated with the collapse of massive stars were studied (Fryer & Woosley 1998; Ruffert & Janka 1999; Mészáros & Rees 1999) and the GRB-Supernova link was discussed (Kulkarni et al. 2000), the wind environment may be important in the hydrodynamic evolution of GRB afterglow. Another problem is whether the burst is spherical or is strongly beamed. Beaming of relativistic blast wave in GRBs was proposed to ease the energy budget (Mészáros, Rees & Wijers 1999). When a collimated flow spreads in the lateral dimension, it encounters more surrounding matter and decelerates faster than in the spherical case (Frail et al. 2001). Now we go further in the consideration of the dynamical evolution by taking into account the wind environment and beaming effect. From Fig. 1, we can see the importance of wind environment. When $r < R_0$, which is the earlier stage of the fireball expansion, the medium in the wind environment is denser than that in the homogeneous medium (ISM). The dense wind environment dominates the deceleration of the fireball. So the value of $\Gamma(r)$ effected by the wind environment declines more rapidly than that by the ISM. Conversely, $r > R_0$ is the later stage of the fireball expansion. The effect of the wind environment is very weak, and the medium is thinner than that of the ISM. In this later stage, the deceleration of the fireball is dominated by the ISM. So the value of $\Gamma(r)$ declines more slowly than that of the ISM.

As mentioned in Section 1, $\varepsilon_e = 1$ and $\varepsilon_e = 0$ are the two limiting cases of hydrodynamic evolution. The curves of $\Gamma(r) \sim r$ determined by other values of ε_e should lie between these two limits. This is verified by the curves in Fig. 2.

Figure 3 shows the beaming effect for different environments. For the hydrodynamic evolution of the beaming effect, two-dimensional solution is needed (Sari, Piran & Halpern 1999). Equation (15) in our text gives a geometric form of the beaming which corresponds to the matter expanding sideways. It is a simple two-dimensional model. When $r < R_0$, the matter has not had enough time (in its own rest frame) to spread sideways, the value of $\Gamma(r)$ declines slowly than in the ISM. When $r > R_0$ and the sideways expansion has become significant, the value of $\Gamma(r)$ declines more drastically than in the ISM.

In this article, we give a detailed course of hydrodynamic evolution. The conclusions are summarized below:

(1) When the value of ε_e is smaller, the evolution curve declines more slowly.

(2) For $r < R_0$, the evolution curve affected by the wind environment declines more rapidly than that by the ISM. For $r > R_0$, the evolution curve affected by the wind environment declines more slowly than that by the ISM.

(3) For $r < R_0$, the evolution curve affected by beaming flow declines more slowly than that in the ISM. For $r > R_0$, the evolution curve affected by beaming flow declines more rapidly than that in the ISM.

(4) The deceleration radius R_0 is of vital importance for the hydrodynamic evolution of GRB afterglow.

Investigating the hydrodynamic evolution is the first step in a comprehensive study of GRB afterglow evolution. On the other physical processes, such as radiation mechanism (Vietri 1997;

Sari, Piran & Narayan 1998; Chiang 1999; Ghisellini, Celotti & Lazzati 1999; Ghisellini et al. 2000), we will give certain results in another paper (Mao & Wang 2001).

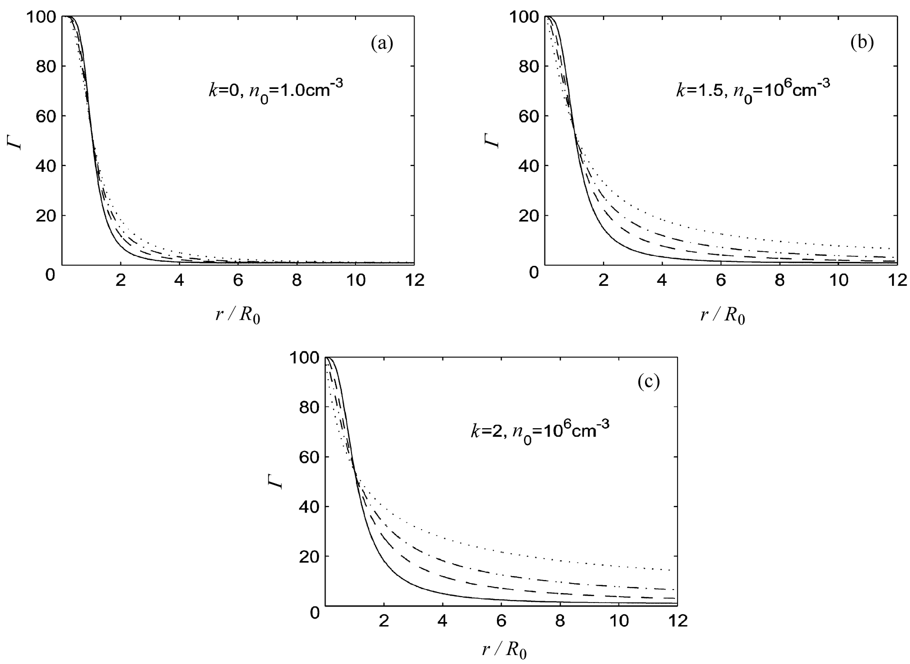

Fig. 3 The hydrodynamic evolution for different environments and for $\varepsilon_e = \frac{1}{2}$. Solid lines for beaming parameter $p = 2$, dashed lines for $p = 1$, dot-dash lines for $p = 0.5$ dotted lines for the isotropic case.

Acknowledgements We would like to thank the anonymous referee for useful comments. This work is supported by National Astronomical Observatories grants (99-5102CA), Chinese Academy of Sciences (CAS). The research is subsidized by the Special Funds for Major State Research Projects (973 Projects).

References

Blandford R. D., Mckee C. F., 1976, Phys. Fluids, 19, 1130
Costa E. et al., 1997, Nature, 387, 783
Castro-Tirado A. J. et al., 1999, Science, 283, 2069
Chevalier R., Li Z. Y., 1999, ApJ, 520, L29
Ching J., 1999, ApJ, 514, 856
Ching J., Dermer C. D., 1999, ApJ, 512, 699
Dai Z. G., 2000, preprint (astr-ph/0008304)
Dai Z. G., Lu T., 1998, MNRAS, 298, 87
Dai Z. G., Lu T., 1999, ApJ, 519, L155
Dai Z. G., Lu T., 2000a, ApJ, 537, 803
Dai Z. G., Lu T., 2000b, A&A, 367, 501
Djorgovski S. G. et al., 1997, Nature, 387, 876

Frail D. A. et al., 1997, Nature, 389, 261
Frail D. A. et al., 2001, preprint (astro-ph/0102282)
Fransson C., Lundquist P., Chevalier R. A., 1996, ApJ, 461, 993
Fryer C. L., Woosley S. E., 1998, ApJ, 502, L9
Fryer C. L., Woosley S. E., Hartmann D. H., 1999, ApJ, 526, 152
Galama T. J. et al., 1999, Nature, 398, 394
Ghisellini G., Celotti A., Lazzati D., 2000, MNRAS, 313, L1
Ghisellini G. et al., 2000, MNRAS, 316, L45
Halpern J. P., et al., 1998, Nature, 393, 41
Huang Y. F. et al., 1998, MNRAS, 298, 459
Huang Y. F., Dai Z. G., Lu T., 1998, A&A, 336, L69
Katz J. I., Piran T., 1997, ApJ, 490, 772
Kulkarni S. R. et al., 1998, Nature, 393, 35
Kulkarni S. R. et al., 1999, Nature, 398, 389
Kulkarni S. R. et al., 2000, preprint (astro-ph/0002168)
Kumar P., Panaitescu A., 2000, ApJ, 541, L9
Mao J. R., Wang J. C., 2001, submitted to CJAA
Mészáros P., Rees M. J., 1993, ApJ, 405, 278
Mészáros P., Laguna P., Rees M. J., 1993, ApJ, 415, 181
Mészáros P., Rees M. J., 1997, ApJ, 476, 232
Mészáros P., Rees M. J., 1999, ApJ, 502, L105
Mészáros P., Rees M. J., Wijers R. A. M. J., 1999, New Astron., 4, 303
Metzger M. R. et al., 1997, Nature, 387, 878
Moderski R., Sikora M., Bulik T., 2000 ApJ, 529, 151
Panaitescu A., Mészáros P., 1998, ApJ, 492, 683
Panaitescu A., Mészáros P., 1999, ApJ, 526, 707
Panaitescu A., Mészáros P., Rees M. J., 1998, ApJ, 503, 314
Rees M. J., Mészáros P., 1992, MNRAS, 258, 41P
Rhoads J. E., 1997, ApJ, 487, L1
Rhoads J. E. 1999, ApJ, 525, 737
Ruffert M., Janka H.-Th., 1999, A&A, 344, 573
Sahu K. et al., 1997, Nature, 387, 476
Sari R., Narayan R., Piran T., 1996, ApJ, 473, 204
Sari R., Piran T., Narayan R., 1998, ApJ, 497, L17
Sari R., Piran T., Halpern J. P., 1999, ApJ, 519, L17
Taylor G. B. et al., 1997, Nature, 389, 263
van Paradijs J. et al., 1997, Nature, 386, 686
Vietri M., 1997, ApJ, 478, L9
Waxman E., 1997, ApJ, 485, L5
Waxman E., 1997, ApJ, 489, L33
Wijers R. A. M. J., Rees M. J., Mészáros P., 1997, MNRAS, 288, L51